Geometry Dependent Superconductive Transition of Nb Nanostructures

Geometry dependent superconductive transition of Nb nanostructures

Ivan De Carlo [1,2], Matteo Fretto [2], Natascia De Leo [2], Gianluca Milano [2]

1- Department of Electronics and Telecommunications, Politecnico di Torino, 10129 Turin, Italy
2- Istituto Nazionale di Ricerca Metrologica (INRiM), 10135 Turin, Italy

Abstract — Recently, superconducting nanostructures gained particular attention due to the visualisation of some intriguing phenomena, such as phase fluctuations, quantum phase slip, and shape resonance in critical temperature, allowing the definition of a tailored superconducting nanodevice with the desired superconducting features and quantum phenomena. A deep investigation into the relationship between superconductivity, low dimensionality, and quantum phenomena should be performed, in order to explain the emergence mechanism of these effects in nanostructures and how superconductivity is affected. In the following, we report on the investigation of the superconductive transition in triangular-shaped Nb pads connecting a Nb nanostripe. As revealed by *R vs T* curves, the superconductive transition is observed to be characterised by two regions: i) a first smooth and wide transition reflecting the continuous reduction in the width of the Nb triangular pads that progressively experience superconductive transition, and ii) a more abrupt transition reflecting the transition of the Nb nanostripe. This work could pave the way concerning the realisation of Nb nanostructures with tunable critical temperature, transition width, and slope.

Index Terms — Niobium, superconducting nanostructures, geometry effect on superconductivity, nanostructured superconducting devices.

I. INTRODUCTION

SUPERCONDUCTIVITY in low-dimensional devices has been investigated since the 1960s with the study of metallic nanofilm, decreasing the thickness of the device from bulk to thin film configuration [1]–[4]. Thanks to technological development, it has become possible to fabricate thinner nanofilms and reduce other dimensions, exploiting the progress in lithography and deposition techniques, realising devices at the nanoscale in all their spatial dimensions [5]. These studies initially brought to light some peculiar phenomena, such as the variation of the main superconducting properties, critical temperature, magnetic field, and energy gap depending on their size, due to the quantum confinement on the superconducting state [6]–[8].

Even though superconductivity is a macroscopically coherent state with a characteristic length, called coherence length, which generally describes the length scale over which the order parameter varies in space, it has been shown that devices approaching this spatial dimension might exhibit variations in their superconducting properties [3], [9], [10]. Therefore, it is possible to define whether the mechanism related to the superconducting transport properties could be considered 2D or 1D, depending on its thickness or diameter compared to the coherence length. However, it is important to notice that this characteristic length is typical of bulk superconductors and that it may vary with the size, going towards a confined structure. Thus, it is not properly accurate to consider it as a constant value that depends only on the material, but it strictly depends on the shape of the superconducting nanostructure [3], [11].

Recently, new fascinating phenomena related to superconducting nanostructures have garnered interest such as thermally activated phase slips, and quantum phase slips, but also the possibility of directly controlling the superconducting current by applying an external electrical field through a planar gate [12]–[15]. As a result of the discovery of these interesting phenomena, novel quantum devices were designed, exploiting the quantum domain of superconductivity in nanostructures. Therefore, attention should be paid to investigate the confinement at the nanoscale in the appearance of these intriguing phenomena and to deeply study the interplay between superconductivity and its size dependence.

In literature many works shed light on the influence of geometry on superconductivity, analyzing how the critical magnetic field is affected, without taking into account investigation on the critical temperature and the superconducting transition [16]–[18]. In particular, device geometry plays an important role in determining superconducting features, at the same time, the geometrical shape of the devices can tune other properties, like the electric field distribution across the device, varying its local intensity, which could be precious for gating applications devices. For this reason, further research into geometric effects on superconductors might be relevant for designing scalable devices towards the nanoscale, in order to avoid undesired effects related to the superconducting transitions, and electric and magnetic field distribution [19].

In this work, we report on the investigation of the superconducting transition of Nb nanostructures, composed of a nanostripe connected by two pads with triangular shapes, and their influence on the superconducting features of the device. The electrical characterisation at low temperature exhibited a peculiar trend on the *R vs T* curve, which showed a superconducting transition that can be divided into two parts: a first wide and smooth resistance drop ascribed to the triangular shape of the Nb pads, due to their continuous reduction in width that gradually

turn each pads section into the superconducting state, and a second one, abrupt and sharp, as a result of the transition of the nanostripe. Several samples with different sizes were analysed, and the influence of the shape of the Nb nanostructures on the superconducting transition was explored, investigating the transition width and the critical temperature linked to the nanostructures size. Our experimental analysis indicated a direct influence of the shape and size of the Nb pads on the superconducting transition, which might shed new light on superconducting circuital design, depending on the desired characteristic which may be tailored by optimising the geometrical shape of the device.

II. EXPERIMENTAL

The fabrication of the Nb nanostructured devices was based on thin film technology, exploiting Electron Beam Lithography (EBL), DC magnetron sputtering, laser lithography, and liftoff procedure for excess material removal. Commercial silicon wafers covered by 500 nm of silicon dioxide (Si-Mat Silicon Materials) were used for the device substrates, due to their high electrical insulating properties. The Nb nanostructured devices nanometric pattern was performed through an EBL system, FEI Quanta3D FEG dual beam (Field Electron and Ion Company) equipped with a Nabity Nanometer Pattern Generator System (JC Nabity Lithography Systems), at an applied voltage of 30 kV, into the surface of poly methyl methacrylate (PMMA) coated samples. The metal deposition was performed by a Kenotec UHV DC magnetron sputtering, at the base pressure of $10-8$ mbar. A 30 nm niobium thin film was deposited on the samples, in an argon atmosphere at a pressure of $5 \times 10-3$ mbar, corresponding to the thickness of the final realised devices. The excess metal was then removed in an ultrasonic acetone bath, able to dissolve the PMMA mask easily, and then dried under nitrogen flow. The wiring procedure was performed similarly to the nanometric part, employing laser lithography (Heidelberg μPG 101), and a 100 nm thick niobium wiring layer.

Field Effect Scanning Electron Microscopy (FESEM) characterization was performed after every fabrication step for the morphological characterisation of the device, and for estimating the size of the Nb nanostructure. The Nb nanostructure was composed of two triangles connected by a 4 μm long nanostripe, as represented in Fig. 1, where a FESEM image of the device is reported. In particular, the two triangular pads are characterised by a maximum width of 5 μm, W_1, kept constant to every device realised, and a minimum width, W_2, corresponding to the nanostripe one, varying from 410 nm down to 250 nm. The Nb nanostructured device is then connected by the four wiring tracks which ensures the possibility to perform a 4-wire characterisation in order to eliminate the contributes in resistance given by tracks and the wiring contacts.

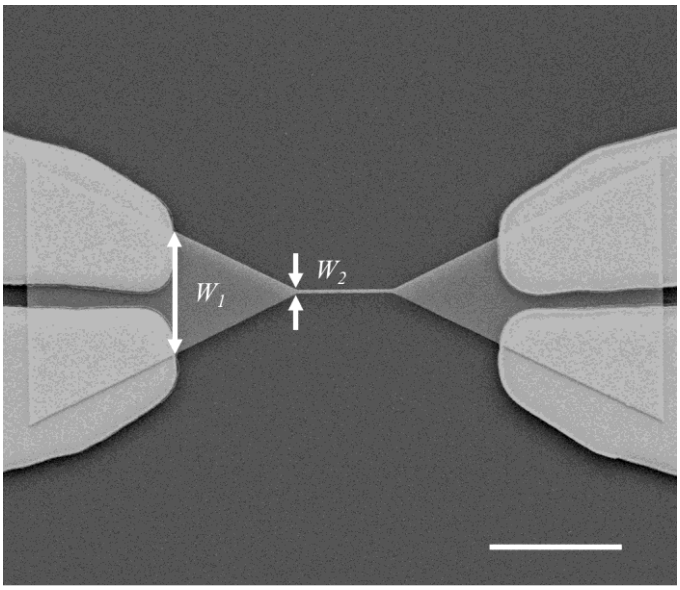

Fig. 1. FESEM image of the Nb nanostructured device (scale bar, 5 μm), with the detail of the two triangles connected by the central nanostripe, and the wiring pads on the side of the device. The two characteristic widths of the triangular pads, W_1 and W_2 are highlighted across the device.

The electrical characterisation was performed in an electromagnetically shielded cryostat, by directly dipping the sample in a liquid helium bath. The sample holder was screwed to the cryoprobe with a Lakeshore DT670 thermometer embedded in the probe. A schematic representation of the measurement setup is reported in Supplementary Figure S1. A Lakeshore 332 controller performed the temperature reading, and its variation was carried out by mechanically moving the cryoprobe over the liquid helium level. A Keithley 6430 amperometer and an Agilent 34401A multimeter were employed for the current bias and the voltage reading. The acquisitions were done through a specific Python code.

III. RESULTS

The Nb nanostructure was designed in order to shrink W_2 from a micrometric scale down to a mesoscopic scale, approaching the order of magnitude of the expected bulk Nb coherence length, approximately 40 nm [20], [21]. The temperature dependence of the resistance, *R vs T*, of the devices was extrapolated by biasing the Nb nanostructures with a constant current of 1 μA and reading the voltage drop across the device while acquiring the temperature from the controller. By inserting the cryoprobe into the cryostat, it was possible to decrease the temperature down to 4.2 K, the liquid helium temperature. This variation was due to a very slow mechanical movement, assuring a complete thermalisation of the system and an accurate estimation of the temperature of the device.

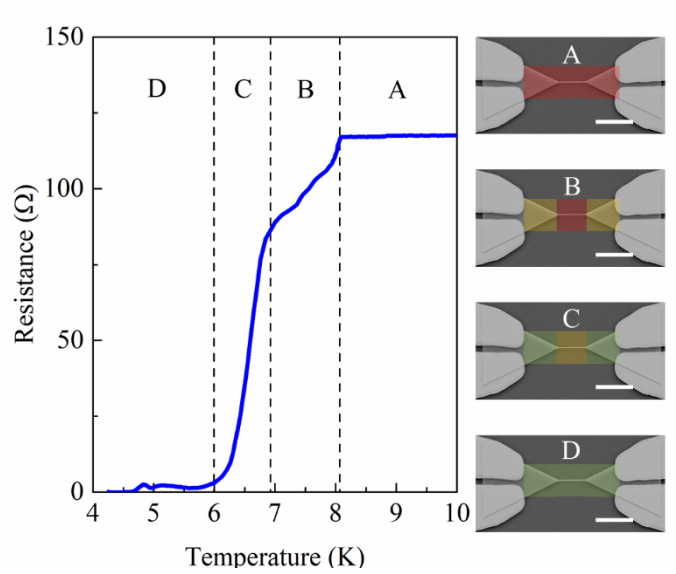

Fig. 2. Temperature dependence of the resistance for a Nb nanostructured device with a minimum width, W_2, of around 320 nm. The curve can be divided into four different sections, with the relative scheme of the part involved in the resistance variation, represented by the FESEM images reported on the right (scale bar, 5 μm), with highlighted in false colour the area involved in the transition: A) normal state, where the entire device acts as a normal metal, exhibiting a finite resistance; B) triangles superconducting transition, where the pads gradually start to become superconducting, decreasing their resistance accordingly to the continuous reduction of their geometrical width, resulting a smooth and wide superconducting transition, while the nanostripe still acts as a normal metal; C) nanostripe superconducting transition, where the nanostripe is starting the resistance decreasing, and the two pads are already to the superconducting state; D) superconducting state, where the entire device has turned to the zero resistance state. The vertical dashed lines separating each region of the curve are guides for eyes, realised to easily distinguish the states that the device encountered during the characterisation. The areas highlighted in false colour correspond to different parts of the curve: the red area to the normal state, the yellow area to the transition, and the green area to the superconducting state.

Fig. 2 depicts a representative characteristic of the temperature dependence of the resistance of a 320 nm (W_2) wide Nb nanostructured device. This curve shows a peculiar trend, which can be divided into four sections. On the right part of the figure, a corresponding FESEM image of the device is reported, highlighting with false colours the area involved in the superconductive transition. The first part (Fig. 2 part A) represents the normal state of the device, which is characterised by a resistance plateau, due to the residual defects in the nanostructure. This plateau continues down to ~ 8 K, which is the critical temperature of a Nb thin film of around 30 nm of thickness [3]. The second part (Fig. 2 part B) shows a wide and broad decrease of the resistance while decreasing the temperature, which is the characteristic behaviour of a

superconducting transition. After a first sudden drop, the resistance starts to decrease slowly and smoothly in region B, with a gentle slope as the temperature decreases. This transition can be ascribed to the transition of the two triangular pads at the sides of the device: these pass from a W_1 of 5 μm down to a W_2 of 320 nm, hence every part of the triangles which became narrower to the previous starts its transition at lower temperature, down to the minimum width of the triangle. Therefore, by lowering the temperature, the pads progressively and continuously transit to the superconducting state, starting from the wider part of the pads down to the narrower. Indeed, the continuous reduction in the width of the triangular pads induces a very wide and smooth resistance drop, due to the progressive transition of the Nb triangles where narrow and narrow sections of the pads transit to the superconducting state while lowering the temperature. The third section (Fig. 2 part C) reports the superconducting transition of the central nanostripe, and it is characterised by a narrower trend compared to the transition in the previous section. Finally, the fourth section (Fig. 2 part D) represents the superconducting state, with a complete decrease in the resistance value below the two transitions. Both the nanostripe transition and the triangles are wider and broad compared to the superconducting transitions present in literature, even for very thin metallic films, which usually are of the order of 100 mK or lower [3]. Although the reduction of the current bias results in an increase of T_C, as expected due to self-heating effects, even at low current bias, *R vs T* still shows features attributable to the superconducting transitions of the triangular pads and the nanostripe (e.g., regions B and C can still be observed, as detailed in Supplementary Figure S2). Note that effects related to problems in sample thermalisation have to be ruled out since cryostats based on liquid helium baths ensure optimal heat exchange and, therefore, we assume that the smooth transition of the triangular pads (Figure 2 part B) is not a measurement artefact, due to the lack of heat transfer, but a self-resistance variation induced by the geometrical variation of the triangular pads. This is supported by the negligible hysteretic behaviour observed in the *R vs T* characteristics during cooling and heating. To prove this hypothesis, *R vs T* curves were performed both during cooling and heating of the sample (see Supplementary Figure S3), resulting in negligible hysteretic behaviour of the two features and confirming that the employed measurement setup ensured any avoidance of thermal inertia. Furthermore, it is important to highlight that the presence of the two superconducting transitions (Figure 2 parts B and C) is strictly related to the configuration of the device based on the Nb nanostructure since measuring only the central Nb nanostripe there would be no evidence of other superconducting transitions besides that of the nanostripe itself (see Supplementary Figure S4).

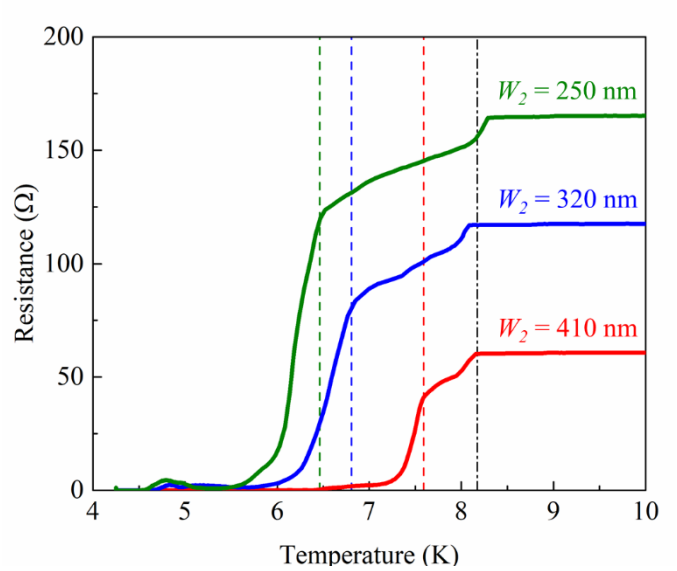

Fig. 3. Temperature dependence of the resistances for three representative Nb nanostructured devices, with three different minimum widths. These curves have a similar trend, with both the triangles and nanostripes superconducting transitions: the first ones became wider while decreasing W_2, starting from the end of the resistance plateau (~ 8 K) and finishing at lower temperatures depending on the curve, while the second ones took place towards lower temperature too. The black dashed and dotted line represents the point where the first transitions start, while the red, blue and green dashed lines represent the point where the first transitions end.

The temperature dependence of the resistance was extrapolated for other devices with different W_2, as reported in Fig. 3, where it is possible to observe three representative curves of three different devices with diminishing widths (from 410 nm down to 250 nm). In fact, these devices have a similar layout, with the two triangular pads at the sides, connected by the central nanostripe, whose W_2varies depending on the device. This affects the triangular pads, which have the W_1 constant to every device, and the W_2 depending on the one of the nanostripe. As an example, we report in Fig. 3 R *vs* T of three different devices characterised by different shapes of the pads (i.e., different W_2). It is worth noticing that the normal state region ends at the same temperature for all of them (~ 8 K) where the first transitions start (black dashed and dotted vertical line of Fig. 3). Small variations of these temperatures may be related to a composition of fabrication artefacts, due to the roughness of the deposited Nb thin film, and to the temperature extrapolation. The first transition has been observed to be wider while shrinking down W_2, while the slope of the transition remained nearly the same. The second thing that it is possible to notice from Fig. 3 is that even the second transition, the nanostripe one, shifts to lower temperatures by decreasing the nanostripe width, which is a behaviour similar to the one of the metallic thin films [3], [22], [23].

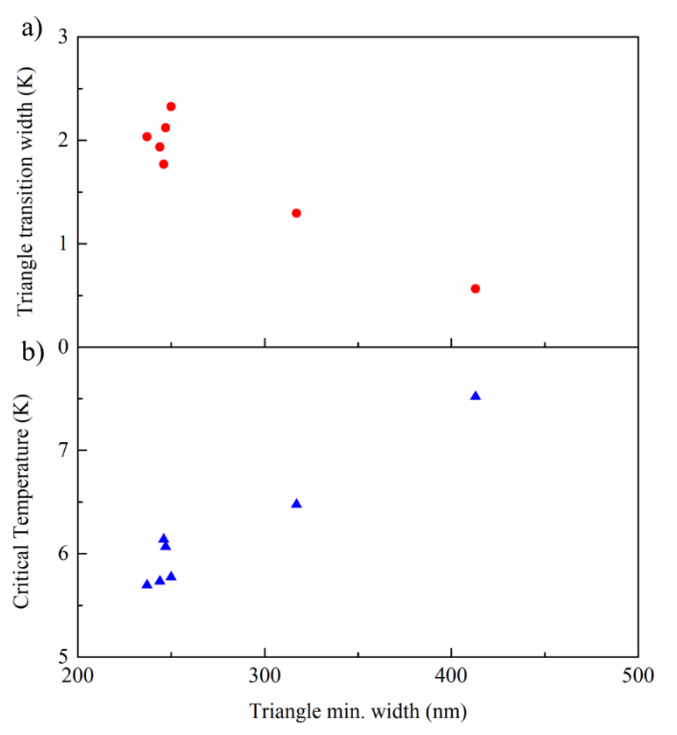

Fig. 4. Characteristics extracted from the temperature dependence of the resistances of the Nb nanostructured devices. a) Superconducting transition width of the Nb pads as a function of the nanostripe width, i.e., minimum width of the device. The transition width increases while getting narrower devices. b) Superconducting critical temperature of the devices as a function of the nanostripe width. The critical temperature decreases while going towards narrower devices.

Since in this case it is non-trivial to define when a transition started and ended, and therefore the criteria based on the 90 % and 10 % of the normal resistance could describe the entire device characteristic, it may not be the appropriate method to analyse only the triangular pads and the nanostripes transitions. The width of the pads superconducting transition (ΔT) was extrapolated by taking the difference of the temperature of the ”elbow” just below the normal state (black dashed and dotted vertical line of Fig. 3) and the temperature of the intersection between the two transitions linear fit (red, blue and green dashed lines of Fig. 3). Fig. 4.a) reports the triangle minimum width W_2, i.e., nanostripe width, dependence of the pads transition width. In particular, the trend of the ΔT shows that it increases while decreasing the minimum width of the Nb nanostructured device.

Furthermore, it is non-trivial even to define the critical temperature (T_C) of the Nb nanostructured device by the previously cited criteria (i.e., the T_C of the transition in Fig. 2 part C), hence it was extrapolated by taking the maximum value of the first derivative of the resistance with respect to the temperature. This method takes the temperature where the slope

of the transition changes its concavity, assuming that as the T_C of the superconducting device. Fig. 4.b) depicts the size dependence of the T_C of the investigated devices, whose values decrease while shrinking down W_2. Even if T_C has an opposite trend depending on W_2 compared to ΔT, these two characteristics give an evidence of the geometrical influence on the superconducting transition, strictly dependent on the thickness and the cross-section of the superconducting device. The mechanism that might explain the suppression of the T_C and the broadening of the triangles transition can be attributed to the decreasing size of the Nb nanostructure, even if it is wider than the expected Nb coherence length. However, the effect of granulometry with a variation in the grain diameters with the decreasing of W_2 and stress effects induced by the lift-off process cannot be excluded [24], [25]. At the same time, these trends are in agreement with the literature related to Nb nanostructured devices, which are subject to a decrease of the critical temperature induced by the confinement effects, similar to the superconducting to insulator transition that has been observed in superconducting thin films [22], [23]. In contrast, other works report deep investigations on Al nanowires, which are subject to an enhancement of the critical temperature [26]. In this context, an in-depth investigation of the physical mechanism underlying the effect of nano-confinement on the superconductivity mechanism is required. Another phenomenon that could be explored, with respect to device geometry, is the variation of device length, which can influence the presence of phase slip centres along the device as the length increases [27]–[29], and could exhibit a Josephson-like behaviour as the length decreases up to the coherence length of the device [30].

IV. CONCLUSION

In summary, we reported on the influence of geometry on the superconducting transition of Nb nanostructures. By considering Nb nanostructures composed of triangular pads connected with a nanostripe, we have shown that this device is characterised by two resistance variations in series: the first one attributed to the triangular pads, affected directly by their gradual reduction in width, which influences the wide and smooth transition, and the second one ascribed to the nanostripe. The extrapolated triangle transition width exhibited a trend related to the pad shape of the device, in particular, the higher was the variation from the larger to the narrower sides of the pad and the higher was the width of the pads transition. A shape dependence was recognised even for the critical temperature related to the nanostripe transition, which decreased its value while going towards lower sizes. We believe that new light should be shed on the relationship between low dimensionality and superconductivity. Further studies are necessary to explain and predict the microscopical mechanism underlying the behaviour of these nanostructures, which still remains a challenge. Future works will focus in-depth on the analysis

of superconducting nanostripes behaviour, trying to reach the quasi-1D configuration, and investigating how the superconducting properties are affected by the 1D geometrical confinement. This work could pave the way for the design and realisation of superconducting nanostructures with tailored transition, with the desired transition width and slope.

ACKNOWLEDGMENTS

This work was carried out at Nanofacility Piemonte, INRiM, a laboratory supported by the " Compagnia di San Paolo" Foundation, and at QR Laboratories, INRiM, a micro and nanofabrication lab.

REFERENCES

[1] T.-C. Chiang, "Superconductivity in thin films," Science, vol. 306, no. 5703, pp. 1900–1901, 2004.

[2] Y.-H. Lin, J. Nelson, and A. Goldman, "Superconductivity of very thin films: The superconductor–insulator transition," Physica C: Superconductivity and its Applications, vol. 514, pp. 130–141, 2015.

[3] N. Pinto, S. J. Rezvani, A. Perali, L. Flammia, M. V. Milo˘sevi´c, M. Fretto, C. Cassiago, and N. De Leo, "Dimensional crossover and incipient quantum size effects in superconducting niobium nanofilms," Scientific reports, vol. 8, no. 1, p. 4710, 2018.

[4] M. Sharma, M. Singh, R. K. Rakshit, S. P. Singh, M. Fretto, N. De Leo, A. Perali, and N. Pinto, "Complex phase-fluctuation effects correlated with granularity in superconducting NbN nanofilms," Nanomaterials, vol. 12, no. 23, p. 4109, 2022.

[5] K. Y. Arutyunov, D. S. Golubev, and A. D. Zaikin, "Superconductivity in one dimension," Physics Reports, vol. 464, no. 1-2, pp. 1–70, 2008.

[6] A. Shanenko, M. Croitoru, and F. Peeters, "Nanoscale superconductivity: Nanowires and nanofilms," Physica C: Superconductivity and its applications, vol. 468, no. 7-10, pp. 593–598, 2008.

[7] Y.-J. Hsu, S.-Y. Lu, and Y.-F. Lin, "Nanostructures of Sn and their enhanced, shape-dependent superconducting properties," Small, vol. 2, no. 2, pp. 268–273, 2006.

[8] S. Bose, P. Raychaudhuri, R. Banerjee, P. Vasa, and P. Ayyub, "Mechanism of the size dependence of the superconducting transition of nanostructured Nb," Physical review letters, vol. 95, no. 14, p. 147003, 2005.

[9] A. Gubin, K. Il'in, S. Vitusevich, M. Siegel, and N. Klein, "Dependence of magnetic penetration depth on the thickness of superconducting Nb thin films," Physical Review B—Condensed Matter and Materials Physics, vol. 72, no. 6, p. 064503, 2005.

[10] K. Kagawa, K. Inagaki, and S. Tanda, "Superconductor-insulator transition in ultrathin Pb films: Localization and superconducting coherence," Physical Review B, vol. 53, no. 6, p. R2979, 1996.

[11] A. Shanenko, M. Croitoru, A. Vagov, and F. Peeters, "Giant drop in the bardeen-cooper-schrieffer coherence length induced by quantum size effects in superconducting nanowires," Physical Review B—Condensed Matter and Materials Physics, vol. 82, no. 10, p. 104524, 2010.

[12] A. Bezryadin, C. Lau, and M. Tinkham, "Quantum suppression of superconductivity in ultrathin nanowires," Nature, vol. 404, no. 6781, pp. 971–974, 2000.

[13] R. S. Shaikhaidarov, K. H. Kim, J. W. Dunstan, I. V. Antonov, S. Linzen, M. Ziegler, D. S. Golubev, V. N. Antonov, E. V. Il'ichev, and O. V. Astafiev, "Quantized current steps due to the ac coherent quantum phaseslip effect," Nature, vol. 608, no. 7921, pp. 45–49, 2022.

[14] C. M. Natarajan, M. G. Tanner, and R. H. Hadfield, "Superconducting nanowire single-photon detectors: physics and applications," Superconductor science and technology, vol. 25, no. 6, p. 063001, 2012.

[15] D. V. Reddy, R. R. Nerem, S. W. Nam, R. P. Mirin, and V. B. Verma, "Superconducting nanowire single-photon detectors with 98% system detection efficiency at 1550 nm," Optica, vol. 7, no. 12, pp. 1649–1653, 2020.

[16] E. Charnaya, C. Tien, K. Lin, C. Wur, and Y. A. Kumzerov, "Superconductivity of gallium in various confined geometries," Physical Review B, vol. 58, no. 1, p. 467, 1998.

[17] J. R. Clem and K. K. Berggren, "Geometry-dependent critical currents in superconducting nanocircuits," Physical Review B—Condensed Matter and Materials Physics, vol. 84, no. 17, p. 174510, 2011.

[18] V. Schweigert and F. Peeters, "Influence of the confinement geometry on surface superconductivity," Physical Review B, vol. 60, no. 5, p. 3084, 1999.

[19] H. Peng, L. Pu, J. Wu, D. Cha, J. Hong, W. Lin, Y. Li, J. Ding, A. David, K. Li et al., "Effects of electrode material and configuration on the characteristics of planar resistive switching devices, " APL Materials, vol. 1, no. 5, 2013.

[20] B. W. Maxfield and W. McLean, “Superconducting penetration depth of niobium,” Physical Review, vol. 139, no. 5A, p. A1515, 1965.

[21] C. Delacour, L. Ortega, M. Faucher, T. Crozes, T. Fournier, B. Pannetier, and V. Bouchiat, “ Persistence of superconductivity in niobium ultrathin films grown on r-plane sapphire,” Physical Review B—Condensed Matter and Materials Physics, vol. 83, no. 14, p. 144504, 2011.

[22] N. Markovi´c, C. Christiansen, A. Mack, W. Huber, and A. Goldman, “Superconductor-insulator transition in two dimensions,” Physical Review B, vol. 60, no. 6, p. 4320, 1999.

[23] V. F. Gantmakher and V. T. Dolgopolov, “Superconductor–insulator quantum phase transition,” Physics-Uspekhi, vol. 53, no. 1, p. 1, 2010.

[24] D. Hazra, M. Mondal, and A. K. Gupta, “Correlation between structural and superconducting properties of nano-granular disordered Nb thin films,” Physica C: Superconductivity, vol. 469, no. 7-8, pp. 268–272, 2009.

[25] S. Bose and P. Ayyub, “A review of finite size effects in quasi-zero dimensional superconductors,” Reports on Progress in Physics, vol. 77, no. 11, p. 116503, 2014.

[26] M. Zgirski, K.-P. Riikonen, V. Touboltsev, and K. Y. Arutyunov, “Quantum fluctuations in ultranarrow superconducting aluminum nanowires,” Physical Review B—Condensed Matter and Materials Physics, vol. 77, no. 5, p. 054508, 2008.

[27] A. Elmurodov, F. Peeters, D. Vodolazov, S. Michotte, S. Adam, F. d. M. de Horne, L. Piraux, D. Lucot, and D. Mailly, “Phase-slip phenomena in NbN superconducting nanowires with leads, ” Physical Review B—Condensed Matter and Materials Physics, vol. 78, no. 21, p. 214519, 2008.

[28] W. Zhao, X. Liu, and M. Chan, “Quantum phase slips in 6 mm long niobium nanowire,” Nano letters, vol. 16, no. 2, pp. 1173–1178, 2016.

[29] A. Bezryadin, Superconductivity in nanowires: fabrication and quantum transport. John Wiley & Sons, 2013.

[30] K. Likharev, “Superconducting weak links,” Reviews of Modern Physics, vol. 51, no. 1, p. 101, 1979.